JACS JOURNAL OF THE AMERICAN CHEMICAL SOCIETY
Article
Cite This: J. Am. Chem. Soc. 2019, 141, 1989−1997
pubs.acs.org/JACS

Mimicking Active Biopolymer Networks with a Synthetic Hydrogel

Marcos Fernández-Castaño Romera,[†,‡,⊥] Robert Göstl,[†,‡,#] Huda Shaikh,[†,‡,¶] Gijs ter Huurne,[†,‡] Jurgen Schill,[†,∥] Ilja K. Voets,[†,‡] Cornelis Storm,[†,§] and Rint P. Sijbesma*[,†,‡]

[†]Institute for Complex Molecular Systems, [‡]Department of Chemical Engineering and Chemistry, [∥]Department of Biomedical Engineering, and [§]Department of Physics, Eindhoven University of Technology, P.O. Box 513, 5600 MB, Eindhoven, The Netherlands

[⊥]SupraPolix BV, Horsten 1, 5612 AX, Eindhoven, The Netherlands

Supporting Information

ABSTRACT: Stiffening due to internal stress generation is of paramount importance in living systems and is the foundation for many biomechanical processes. For example, cells stiffen their surrounding matrix by pulling on collagen and fibrin fibers. At the subcellular level, molecular motors prompt fluidization and actively stiffen the cytoskeleton by sliding polar actin filaments in opposite directions. Here, we demonstrate that chemical cross-linking of a fibrous matrix of synthetic semiflexible polymers with thermoresponsive poly(*N*-isopropylacrylamide) (PNIPAM) produces internal stress by induction of a coil-to-globule transition upon crossing the lower critical solution temperature of PNIPAM, resulting in a macroscopic stiffening response that spans more than 3 orders of magnitude in modulus. The forces generated through collapsing PNIPAM are sufficient to drive a fluid material into a stiff gel within a few seconds. Moreover, rigidified networks dramatically stiffen in response to applied shear stress featuring power law rheology with exponents that match those of reconstituted collagen and actomyosin networks prestressed by molecular motors. This concept holds potential for the rational design of synthetic materials that are fluid at room temperature and rapidly rigidify at body temperature to form hydrogels mechanically and structurally akin to cells and tissues.

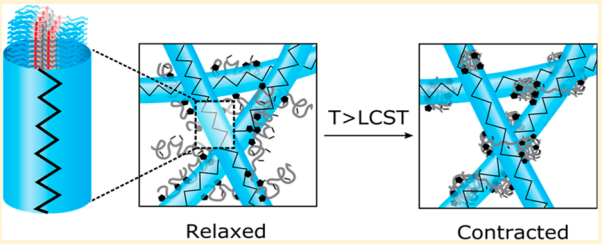

INTRODUCTION

Filamentous biomaterials, such as the actin cytoskeleton, collagen-based extracellular matrix, and fibrin blood clots, are three-dimensional, interlinked meshworks of protein biopolymers. They are the scaffold of life, shaping and supporting our cells and tissues. In order to do so in a robust and adaptive manner, their architecture (the spatial arrangement of and connections between fibers) is highly dynamic, both in terms of constituent polymers, which grow, shrink, and reorient,[1−3] and in terms of connections, which relocate, dissociate, and (re)bind.[4−6] Concomitantly, the mechanical response of a given architecture may be actively amplified; previous work in cells, tissues, and reconstituted protein meshworks has demonstrated the capacity of external and internal stresses and strains to change the stiffness of a material by orders of magnitude.[4,7,8] One such active control modality consists of the exertion of small and highly localized forces on a polymer network. At subcellular scales, these forces may be imparted by molecular motors;[9−13] in the extracellular matrix they arise from contractile cells (platelets and smooth muscle cells (SMCs)).[14−16] This microscopic pinching is at the root of a number of highly functional biomechanical behaviors: motors may prompt flow and fluidization of the cellular cytoskeleton to permit cell motility;[10,13,17,18] SMC-mediated forces exert significant prestress on the aortic wall, which strengthens it by prompting remodeling and deposition of additional collagen.[16,19] Platelet-mediated forces prompt the collapse and contractility of blood clots. Clearly, such responsive functionality allows biopolymeric materials to robustly perform and respond at different length scales and to a variety of external cues.

Inspired by these biological regulatory mechanisms, recent work of Rowan and co-workers[20] successfully exploited the potential of lower critical solution temperature (LCST) polymers to augment the mechanical response of composite materials upon induction of coil−globule collapse. In their work, stiff cellulose nanocrystals (CNCs) were grafted with thermoresponsive poly(oligo(ethylene glycol)monomethyl ether (meth)acrylates) (POEG(M)A) and embedded within a soft poly(vinyl acetate) (PVAc) rubbery matrix. Gels made from these materials reversibly change modulus with heating and cooling. Stiffening arises from the formation of a percolated network of stiff CNC fibers brought into physical contact via the collapse of the thermoresponsive element, and softening to recover the original modulus is brought about by rehydration of the collapsed globules below their LCST point.

In this work, we combine the potential of polymers that exhibit LCST behavior to induce local contractile forces with the strain-stiffening response intrinsic to meshworks of

Received: October 8, 2018
Published: January 12, 2019

DOI: 10.1021/jacs.8b10659
J. Am. Chem. Soc. 2019, 141, 1989−1997

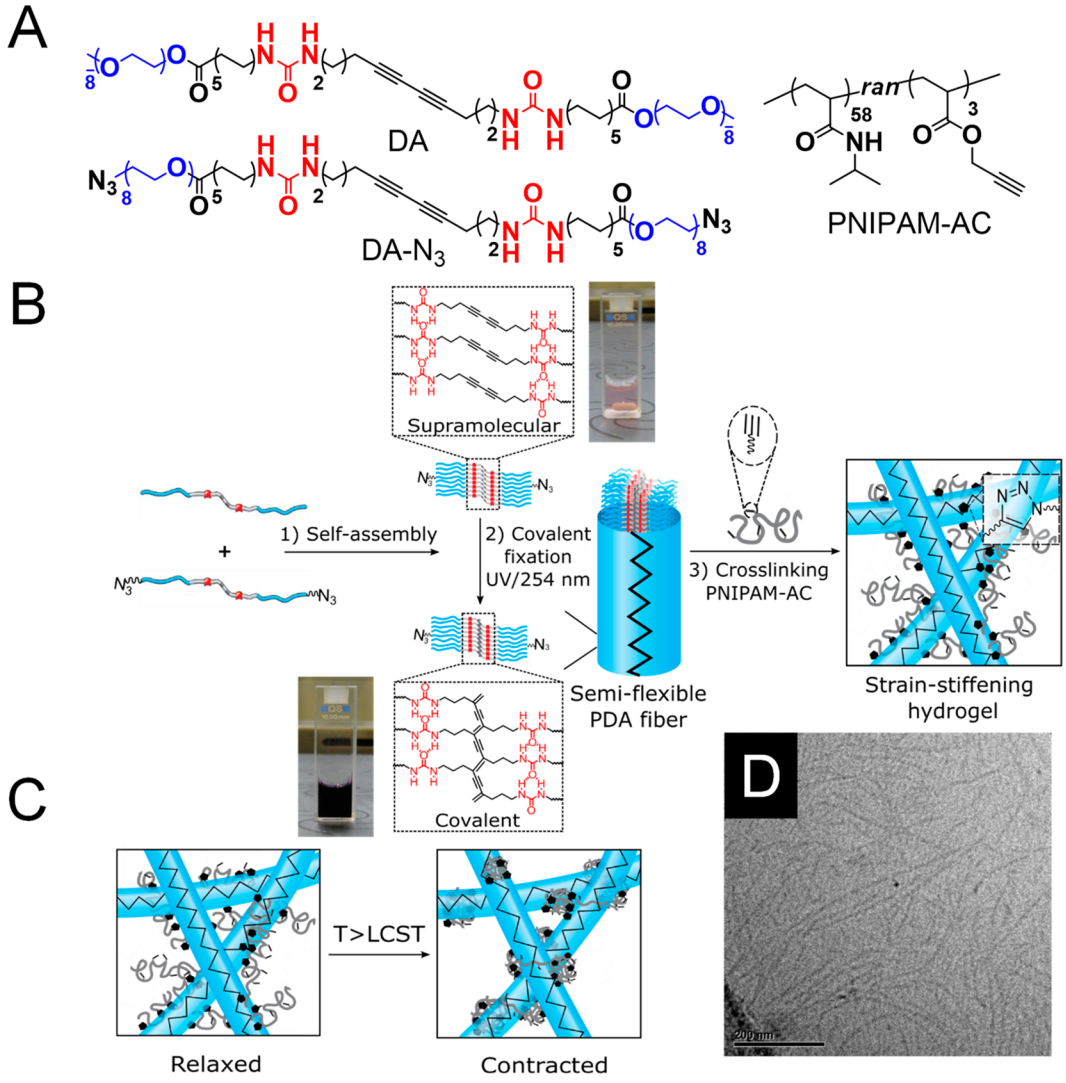

Figure 1. Molecules and methods used to construct biomimetic active polymer networks. (A) Molecular structure of the fiber-forming diacetylene bis-urea bolaamphiphile DA, its azide-functionalized analogue DA-N_3, and the linear, thermoresponsive PNIPAM-AC linker. (B) Hierarchical self-assembly through intermolecular H-bonding and hydrophobic interactions of DA-N_3 and DA followed by topochemical polymerization of the assembled diacetylene groups into PDA fibers. Covalent fixation results in strongly colored solutions due to the formation of a π-conjugated ene-yne covalent framework. The fiber cross-section consists of 9 or 10 ribbons of aggregated molecules. Chemical cross-linking with linear PNIPAM-AC via CuAAC reaction into strain-stiffening networks with triazole cross-links. (C) Internal stress generation within the fibrous PDA matrix mediated by PNIPAM-AC coil-to-globule transition above its LCST. (D) Cryo-electron micrograph (cryo-EM) of PDA fibers in water (1 mM). Scale bar: 200 nm.

semiflexible polymers.[21] We demonstrate that the induction of coil−globule collapse of poly(*N*-isopropylacrylamide) (PNIPAM) chains that cross-link semiflexible fibers of poly(diacetylene) bis-urea bolaamphiphiles (PDA) (Figure 1) dramatically changes the linear mechanical response, rigidifying a previously fluid system to produce a robust and elastic material. Moreover, we show that in the nonlinear deformation regime universal strain-stiffening occurs, with a power-law stiffening exponent that matches that of collagen networks. This process happens at a constant overall volume. With this work, we engineer a strain-stiffening soft material that shows a temperature-controlled rigidification induced by local strain.

RESULTS AND DISCUSSION

In previous work, we introduced diacetylene bisurea bolaamphiphiles (DA) (Figure 1A) as a versatile motif to construct strain-stiffening hydrogels.[22] In water, DA molecules self-assemble through an interplay of intermolecular urea−urea hydrogen bonds (that guide the 1D assembly process) and hydrophobic interactions into semiflexible fibers (Figure 1D). The so-formed fibers can be mechanically reinforced with covalent bonds via photopolymerization of the assembled diacetylene groups into PDA fibers with an associated change in optical properties owing to the formation of a π-conjugated framework.[23] In aqueous media, PDA fibers have an average contour length of 157 nm, persistence length of 280 nm, and a cross-sectional diameter of 3.3 nm.[22] Further analysis revealed that PDA fibers' cross-section contains 9 or 10 ribbons of aggregated molecules (Figure 1B), thereby imparting the bending stiffness needed to be applied as protein mimics. Gelation of PDA fibers was achieved by introducing cross-linkable analogues (DA-N_3) into the fiber-forming DA host before the covalent fixation step. Thus, clicking of azide- and acetylene-labeled PDA fibers by means of a ligand-accelerated

DOI: 10.1021/jacs.8b10659
J. Am. Chem. Soc. 2019, 141, 1989−1997

Cu-catalyzed cycloaddition reaction (CuAAC)[24] yielded strain-stiffening gels without an increase in fiber dimensions (i.e., no additional bundling) upon chemical cross-linking.[22] In the current work, PDA fibers functionalized by incorporation of 20 mol % DA-N_3 were chemically cross-linked with a PNIPAM copolymer containing 5% propargyl acrylate residues (PNIPAM-AC). The reaction afforded fibrous gels covalently interlinked with a thermoresponsive linear polymer as schematically depicted in Figure 1B.

Synthesis and Characterization of PNIPAM-AC. PNIPAM-AC was prepared via reversible addition−fragmentation chain-transfer (RAFT) copolymerization of NIPAM and trimethylsilyl (TMS)-protected propargyl acrylate. TMS protection was carried out in order to prevent unwanted branching and eventual cross-linking of the individual chains by polymerization of the somewhat polymerizable terminal alkyne moieties.[25] In the final step, the TMS groups were removed with tetra-*n*-butylammonium fluoride (TBAF) to give a linear polymer with an average molecular weight of M_n = 6.96 kDa and a dispersity of $Đ_M$ = 1.08 (see Supporting Information). Thus, each polymer chain consists of 62 repeat units on average, of which 3.1 are propargyl acrylate residues. The cloud point of PNIPAM-AC in water was studied by measuring the transmittance at 600 nm in a UV−vis spectrophotometer over a temperature range from 20 to 35 °C. Solutions became turbid at ca. 27 °C at a concentration of 5 mg mL^{-1}, and the drop in transmittance shifted toward lower temperatures at increased polymer concentration (Figure 2).

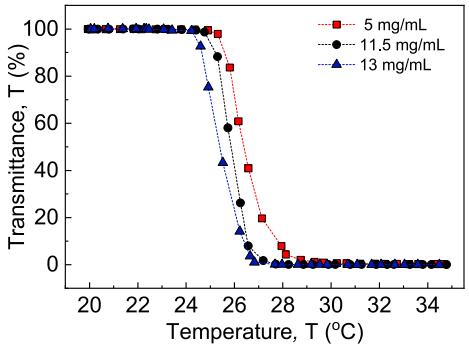

Figure 2. Cloud point temperatures ($T_{CP(50\%)}$) of PNIPAM-AC coils in water measured at different polymer concentrations.

The cloud point temperature was taken as the temperature at which transmission had dropped by 50% ($T_{CP(50\%)}$) and was lower than the literature value of 32 °C,[26] likely due to the incorporation of a hydrophobic co-monomer, as has been previously reported for other PNIPAM copolymers.[27,28] Increasing the amount of propargyl acrylate to 10 mol % in the monomer feed rendered the polymers insoluble in water, which limited the degree of functionalization of PNIPAM-AC.

Gelation and Thermal Analysis of the Hydrogels. Chemical cross-linking was initiated by adding the catalyst mixture to an aqueous solution of polymerized PDA (containing 20 mol % DA-N_3) fibers and PNIPAM-AC. Solutions were immediately transferred to the rheometer, where the gelation process was monitored by measuring the change in moduli at a constant temperature of 20 °C with small-amplitude oscillatory strain (1%) until a constant value of the elastic modulus G' was reached (Figure S3). Concurrently, networks below the critical connectivity threshold (no measurable storage modulus G' at 20 °C) were allowed to react for ca. 10 h in the rheometer prior to analysis.

Thermal analysis was performed by subjecting the hydrogels to a linear temperature ramp from 20 to 55 °C while continuously recording the change in moduli with small-amplitude oscillatory strains. At room temperature, increasing the concentrations at a fixed ratio of acetylene to azide groups, [PNINAM-AC]/[DA-N_3] = 0.78, produced progressively stiffer materials with moduli G' ranging from 2 to 200 Pa in the concentration range between 13 and 23 mg mL^{-1} (Figure 3A). Below 10 mg mL^{-1} PDA however, the storage modulus of

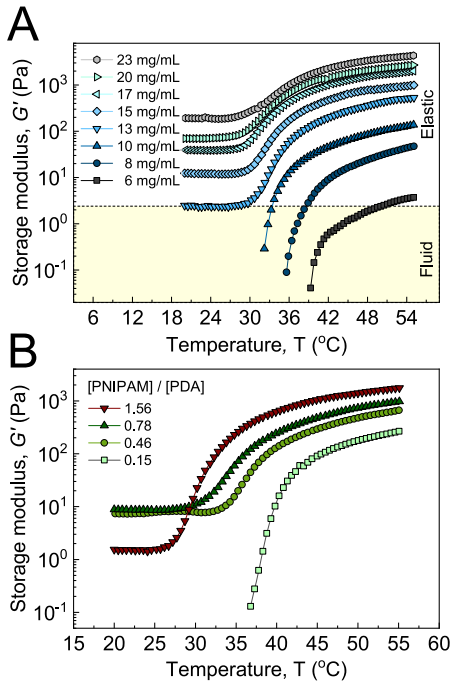

Figure 3. Thermal stiffening of PDA/PNIPAM-AC hydrogels. (A) Linear storage modulus G' vs temperature recorded by applying γ = 1% and ω = 6.28 rad s^{-1} at a linear heating rate of 1.25 °C min^{-1} for different PDA (20 mol % DA-N_3) concentrations cross-linked using a fixed molar ratio of acetylene to azide groups, [PNIPAM-AC]/[DA-N_3] = 0.78. The yellow region represents the concentration threshold required for connectivity at 20 °C. (B) G' vs T for 15 mg mL^{-1} PDA (20 mol % DA-N_3) hydrogels cross-linked using different [PNINAM-AC]/[DA-N_3] molar ratios.

the networks could not be probed at room temperature (yellow region of Figure 3A). Within this concentration regime, all networks remained in the liquid state below the LCST of PNIPAM-AC and formed hydrogels able to support their own weight after placing the sample tubes in a hot water bath at 55 °C. Rigidification of the gels took place within seconds without macroscopic shrinkage, nor was water expelled from the hydrogel (Figure S4). Samples remained in the gel state even weeks after returning to room temperature. Rheology during the T-ramp showed an increase of G' by more than 2 orders of magnitude with the stiffening setting in at temperatures slightly above the measured cloud point of PNIPAM-AC in water (Figure 3A) and gradually shifting toward lower temperatures at higher polymer concentrations. In line with this observation, although "free" PNIPAM-AC exhibits a characteristic concentration-dependent shift in cloud point, this effect was enhanced in the presence of PDA fibers

DOI: 10.1021/jacs.8b10659
J. Am. Chem. Soc. 2019, 141, 1989−1997

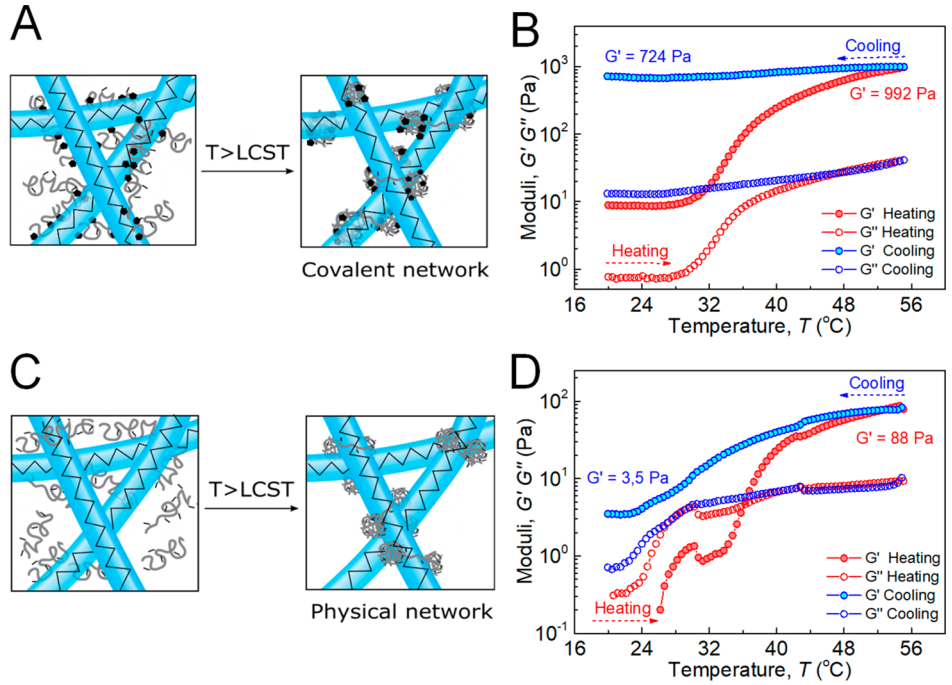

Figure 4. Proposed mechanism of PDA/PNIPAM-AC stiffening transition. (A) Mechanism proposed for the stiffening transition at a constant overall volume observed in a covalently cross-linked PDA/PNIPAM-AC network. (B) Storage (G') and loss (G'') moduli vs temperature at γ = 1% and ω = 6.28 rad s^{-1} and a heating/cooling rate of 1.25 °C min^{-1} for a network consisting of 15 mg mL^{-1} PDA (20 mol % DA-N_3) cross-linked with PNIPAM-AC using a [PNINAM-AC]/[DA-N_3] = 0.78 molar ratio. (C) Sol−gel transition via formation of a physical network lacking chemical cross-links between PDA and PNIPAM-AC. (D) 15 mg mL^{-1} PDA mixed with PNIPAM-AC using a [PNINAM-AC]/[DA-N_3] = 0.78 molar ratio in the absence of added catalyst. Below 30 °C, the data are of limited accuracy, as they are dominated by inertia effects with a raw phase angle above 170° (Figure S10).

screening the globules. For instance, while a 5 mg mL^{-1} PNIPAM-AC solution became turbid at 25 °C (in Figure 2), the transition was shifted to ca. 35 °C for the same concentration of PNIPAM-AC when cross-linked to 10 mg mL^{-1} PDA fibers (blue up-triangles in Figure 3A). Although kinetic effects can be excluded as the main source of this delayed cloud point—given the fast rigidification observed when samples were placed in a hot water bath compared to the experimental time scale of the T-ramp, i.e., 28 min—similar shifts in LCST have been reported in thermoresponsive POEG(M)A polymers when grafted to CNCs and have been ascribed to the hydrophilic nature of the CNC.[20]

The significant increase in G' prompted by PNIPAM-AC coil-to-globule transition seen in Figure 3 can be related to the isotropic nature of the induced deformation, whereby PNIPAM-AC collapse pulls on PDA fibers regardless of their initial orientation. By contrast, stiffening due to anisotropic shear stress preferentially recruits fibers aligned in the direction of the imposed strain.[21,29,30] The approximately 100-fold increase in modulus found for the PNIPAM-containing system is reminiscent of filamin A (FLNa)-cross-linked F-actin networks isotropically stressed via contractile forces imparted by embedded myosin II motor proteins or of fibrin in blood clots stiffened by contractile platelet-mediated forces.[12,13,31−33]

To study the effect of the ratio of acetylene to azide groups on the macroscopic properties of the hydrogels, solutions containing 15 mg mL^{-1} PDA fibers (containing 20 mol % DA-N_3) were cross-linked using varying concentrations of PNIPAM-AC ranging from 1.5 to 15 mg mL^{-1}, resulting in acetylene to azide ratios between 0.15 and 1.56. Cross-linking at a ratio of 0.15 produced a fluid material of which G' could not be probed at 20 °C (Figure 3B, light green squares). Upon increasing the ratio of acetylene to azide groups to 0.39, the G' of the hydrogels crossed the threshold required for connectivity. When the ratio was increased to 1.55, G' was lowered again. We conjecture that the modulus decreases at high ratios because when acetylene groups are present in excess, a larger fraction of PNIPAM molecules react with just one of their acetylene groups, and the extent of interfiber cross-linking is reduced. The cross-linker to fiber ratio also influences the thermal stiffening of the gels. The storage modulus of the different gels of Figure 3B was measured as a function of temperature during a linear T-ramp from 20 to 55 °C. The data show that, for networks above the connectivity threshold, the net increase in G' resulting from PNIPAM-AC collapse increases with increasing cross-linker to fiber ratios. Specifically, at a 1.55 ratio of acetylene to azide groups, G' increases more than 3 orders of magnitude, from 1.5 Pa at 20 °C to 1790 Pa at 55 °C. Similar trends have also been observed in reconstituted actomyosin networks where the magnitude of the stiffening response is coupled to the relative amount of force-generating and cross-linking proteins. Hence, high [myosin]/[actin] or high [FLNa]/[actin] molar ratios induce stronger local tension on the filaments, resulting in higher degrees of macroscopic stiffening.[12,13,34,35]

To compare the linear storage modulus of PDA/PNIPAM hydrogels to those of a "bare" PDA network lacking a force-generating linker as well as intrafiber cross-links, a direct cross-linking approach recently reported by us was employed (Figure S6).[36] Thus, 15 mg mL^{-1} PDA/DA-N3 and PDA-DA-AC fiber solutions (each containing 20 mol % cross-linkable molecules) were mixed after the covalent fixation step and chemically

DOI: 10.1021/jacs.8b10659
J. Am. Chem. Soc. 2019, 141, 1989−1997

cross-linked. Since covalent fixation anchors the monomers to the fibers, interfiber migration of reactive groups is prevented. Accordingly, all cross-links effectively connect two different fibers, and the number of cross-links that contribute to the network's modulus is maximized. This network was found to have a linear storage modulus of 25 Pa, just above the value (9 Pa) of the stiffest network attained using PNIPAM-AC at a [PNIPAM-AC]/[DA-N_3] = 0.78 molar ratio, indicating that in the PNIPAM-containing network, cross-link density at an optimized cross-linker to fiber ratio is near the maximum value.

Irreversibility of the Thermally Induced Stiffening Transition. To identify the underlying mechanisms governing the stiffening of PDA/PNIPAM-AC networks, the moduli of the gels were monitored as they were heated to 55 °C and subsequently cooled back to 20 °C before and after chemical cross-linking of a solution containing 15 mg mL^{-1} PDA/DA-N_3 fibers and 7.5 mg mL^{-1} PNIPAM-AC (Figure 4A,C). For chemically cross-linked gels (Figure 4A,B), heating above the LCST of PNIPAM-AC prompts a 100-fold increase in G' that infers strong pulling of PNIPAM-AC on PDA fibers as the linker undergoes a coil-to-globule transition. After cooling back to 20 °C, the hydrogel remained in a stiffened state in line with previous observations showing an irreversible fluid−gel transition after removing the gel from the heating source (Figure S4). Interestingly, a solution of PDA fibers and PNIPAM-AC coils without covalent connections between the two components was also found to transition from fluid to gel, featuring a crossover of G' and G'' at around 35 °C (Figure 4D). These results suggest that, much like in composite CNC/PVAc/POEG(M)A networks reported by Cudjoe et al.,[20] the collapse of the thermoresponsive linker brings PDA fibers into physical contact, creating a percolating network even in the absence of chemical cross-links. The storage modulus of the physical gel after cooling back to room temperature was over 2 orders of magnitude lower than in the cross-linked material, indicating that, while the formation of physical connections is sufficient to form an elastic material, covalent cross-links strongly increase network connectivity, resulting in much stiffer gels at the same fiber concentration. On cooling back to room temperature, the physical hydrogel relaxes part of the built-up stress as inferred from a decrease in modulus likely due to PNIPAM chains loosening their grip around the fibers as they swell below their LCST. By contrast, in both CNC/PVAc/POEG(M)A composites and biopolymer actin/myosin II networks, full recovery of the original stiffness is achieved after cessation of the active contraction.[13,17,20,31] A possible explanation to account for the contrasting irreversibility found in PDA/PNIPAM-AC networks involves a poorly reversible interaction between the hydrophobic cores of two fibers, which are brought together upon heating above the LCST of the PNIPAM component, but do not detach form each other when the PNIPAN chains swell again upon cooling.

Mesoscale Structural Characterization of the Hydrogels. Relevant insights into the structure of chemically and physically cross-linked PDA/PNIPAM-AC networks were obtained using small-angle X-ray scattering (SAXS). SAXS experiments were performed both below and above the LCST of PNIPAM-AC to probe the topology of both systems (Figure 5). Scattering of the physical gel at 20 °C is very similar to the sum of the scattering of the separate components, showing that there is little interaction between the two polymers (Figure 5A). In the covalent gel at the same temperature, there is excess scattering intensity at low q values with a power law

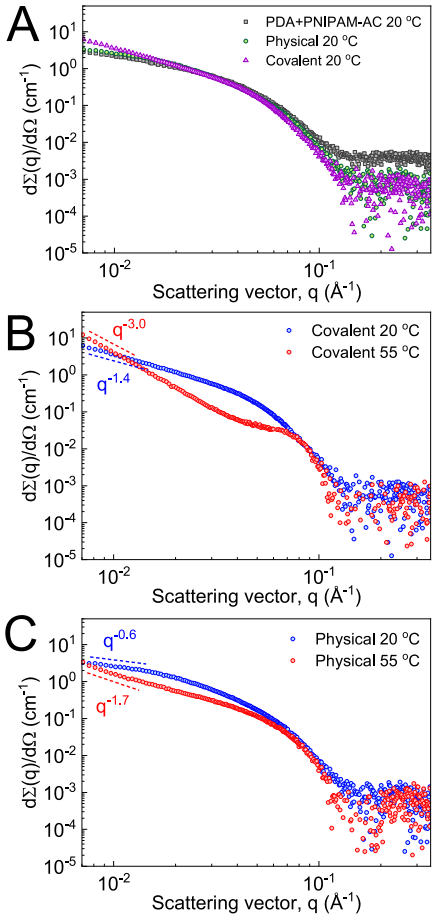

Figure 5. Small-angle X-ray scattering profiles of un-cross-linked physical mixture and covalently cross-linked PDA/PNIPAM-AC (20 mol % DA-N_3) gels at 15 mg mL^{-1} PDA and PNIPAM-AC. Molar ratio [PNINAM-AC]/[DA-N_3] = 0.78. (A) Comparison of the scattering intensities of the physical gel and the covalent gel with the sum of the scattering intensities of the separate components. (B) Covalently cross-linked gel at 20 and 55 °C. (C) Physical mixture at 20 and 55 °C.

exponent that has increased from −1 to −1.5 (purple up triangles in Figure 5A). This indicates structural heterogeneities at mesoscopic length scales (>±15 nm), in line with a calculated mesh size of 82 nm at this concentration (Table S2). Upon heating to 55 °C, when the thermosensitive PNIPAM-AC chains collapse above their LCST, the excess forward scattering intensity and power law exponents increase for both the chemically (Figure 5B) and physically (Figure 5C) cross-linked hydrogels as the heterogeneities herein become more pronounced. In the high q-region, the SAXS profiles recorded above and below the LCST overlay, indicating that the cross-sectional diameter of the PDA fibers in the hydrogels remains fixed at approximately 3 nm. Interestingly, a correlation peak arises exclusively in the covalently cross-linked hydrogel above the LCST. Fitting with a model to describe aggregation in polymer solutions,[37] which has also been employed to describe peptide hydrogels,[38] gives a correlation length of 1.2 nm, smaller than the diameter of the fibers (Figure S8). Tentatively, we attribute this feature to the emergence of small domains composed of collapsed PNIPAM-AC globules.

Nonlinear Mechanics of Prestressed PDA/PNIPAM Hydrogels. To more accurately capture the mechanical response of PDA/PNIPAM-AC networks stiffened via

DOI: 10.1021/jacs.8b10659
J. Am. Chem. Soc. 2019, 141, 1989−1997

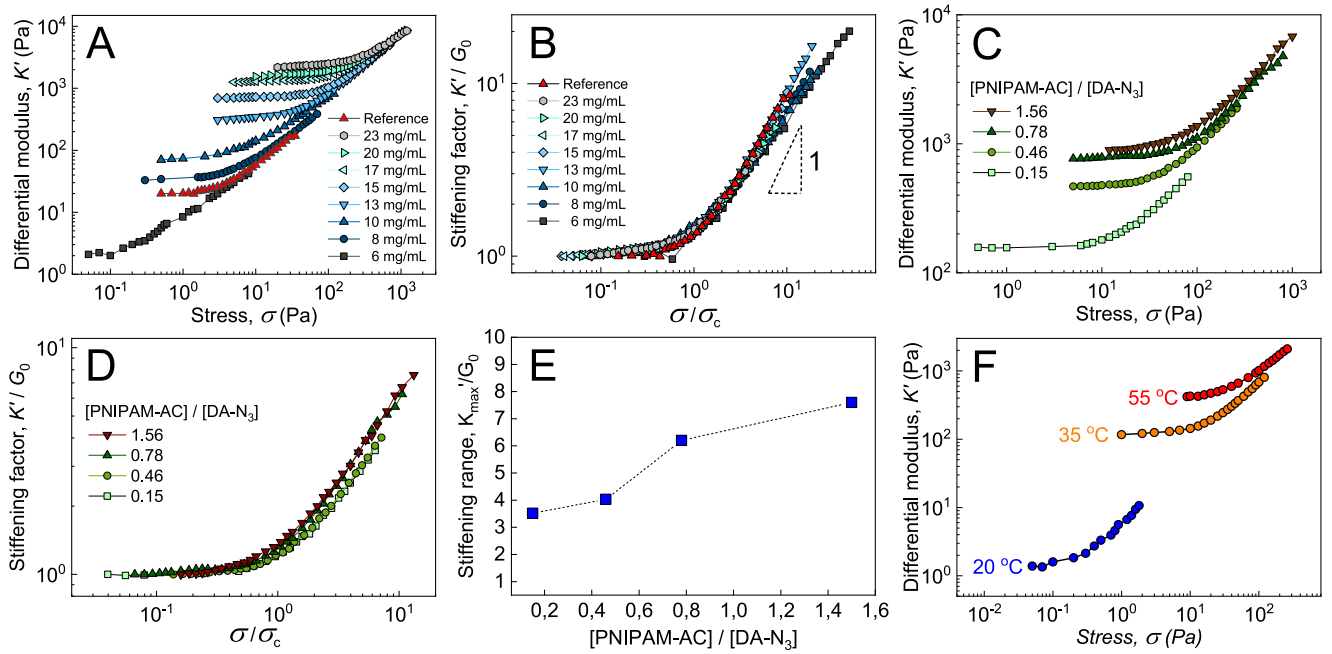

Figure 6. Nonlinear mechanical response of PDA/PNIPAM-AC hydrogels to externally applied shear stress after heating the gels to 55 °C and cooling back to 20 °C. (A) Differential modulus K' plotted against stress σ for different concentrations of PDA cross-linked using a fixed molar ratio [PNINAM-AC]/[DA-N_3] = 0.78 obtained from prestressed gels of Figure 3A. (B) Plot of K' vs stress σ with K' normalized to G_0 and σ normalized to σ_c, showing collapse onto a single master curve with $K' \propto \sigma^1$ at high σ. (C) K' vs σ measured at 20 °C for 15 mg mL^{-1} PDA cross-linked using varying [PNINAM-AC]/[DA-N_3] molar ratios obtained from prestressed gels of Figure 3B. (D) Plot of K' vs stress σ with K' normalized to G_0 and σ normalized to σ_c, showing collapse onto a single master curve. (E) Stiffening factor at failure K'_{max}/G_0 plotted against [PNINAM-AC]/[DA-N_3] molar ratio. (F) Differential modulus K' plotted against stress σ for a PDA hydrogel (12 mg mL^{-1}) cross-linked using a [PNINAM-AC]/[DA-N_3] = 0.78 molar ratio, measured at different temperatures. The gel was brought to its σ_{max} only in the last run at 55 °C.

PNIPAM-AC collapse in Figure 3 under externally applied shear stress, a benchmarked rheological prestress protocol was applied.[39] Accordingly, the differential modulus K (the elastic part of which relates the change in stress with strain, $K' = \delta\sigma/\delta\gamma$) was measured by parallel superposition of an oscillatory and a steady prestress σ. The stiffness—quantified by K'—of most synthetic hydrogels based on flexible polymer chains is constant at biologically relevant stresses.[21] By contrast, gels reconstituted from most intra- and extracellular filamentous proteins are known to exhibit two distinct regimes: a low-stress linear regime, where K' is equal to the plateau storage modulus G_0, and a high-stress nonlinear regime, where K' increases with σ as $K' \propto \sigma^m$, with m being the so-called stiffening exponent.

K' vs σ data were recorded after applying a T-ramp from 20 to 55 °C (in Figure 3) and cooling back to 20 °C. Since the stiffening transition for covalently cross-linked networks was almost fully irreversible, the moduli of the gels at 20 °C were nearly identical to the values at 55 °C. Thus, stiffened PDA/PNIPAM networks from Figure 2B were subjected to a range of steady prestress σ at 20 °C. All networks exhibited an apparently linear response over a concentration-dependent range of applied σ (Figure 6A). However, at a characteristic critical stress (σ_c) the moduli of the gels begins to increase. Strikingly, a 4-fold increase in PDA concentration at a [PNIPAM-AC]/[PDA] ratio of 0.78 combined with an externally applied stress raises the plateau storage modulus from 2 Pa to 10 kPa, nearly 4 orders of magnitude. Concomitantly, the stress at failure (σ_{max}) increases with concentration by 3 full decades. For the highest PDA concentration, σ_{max} reaches a value of 1.3 kPa, vastly surpassing the maximum stress of synthetic polyisocyanopeptides (PICs)-based biomimetic gels, i.e., $\sigma_{max} \approx 40-100$ Pa, where the solubility range of PIC polymers is considerably narrower.[40,41] To quantify the dependence on c of both G_0 and σ_c, scaling analysis was performed and revealed a $G_0 \propto c^{5.1}$ and $G_0 \propto \sigma_c^{5.1}$ relationship over the whole c range studied (Figure S9). Such scaling differs from the typical square dependence found in both theoretical and literature values.[7,40,42,43] We hypothesize that the principal effect causing the strong concentration dependence of G_0 is, among other factors, the concentration-dependent ratio of intrafiber to interfiber cross-linking. Additionally, we warn against overinterpretation, as we do not have scaling data over even a single decade and therefore cannot rule out that the observed dependence is a crossover effect.

The nonlinear mechanics of PDA/PNIPAM hydrogels were compared to those of the "bare" PDA reference network lacking a thermoresponsive linker as well as intrafiber cross-links (Figure S6A). Such networks, obtained by cross-linking fibers with either 20 mol % DA-AC or DA-N_3 analogues showed identical stiffening behavior to the PDA/PNIPAM hydrogels (Figure 6A; red triangles), indicating that the nonlinear elastic response of these materials is exclusively governed by the semiflexible matrix of PDA fibers resisting bending and elongation.

All curves in Figure 6A, including the reference curve of the bare PDA network, were reduced to a single master curve by normalizing K' to its value in the low-stress linear regime G_0 and by normalizing σ to σ_c (Figure 6B). The master curve exhibits power-law dependence $K' \propto \sigma^1$ above σ_c. This value of the stiffening exponent (m) features universally in biopolymer materials at all length scales. In subcellular scales, $m = 1$ has been reported for reconstituted, active networks of FLNa-cross-linked actin stiffened by myosin II.[13] At whole-cell scales,

DOI: 10.1021/jacs.8b10659
J. Am. Chem. Soc. 2019, 141, 1989−1997

m = 1 is robustly seen in entire fibroblasts.[44] Macroscopically, m = 1 is likewise reported for extracellular hydrogels of reconstituted type I collagen.[45] This match between PDA/PNIPAM-AC hydrogels and filamentous biomaterials highlights the biomimetic nature of these materials.

To assess the effect of [PNINAM-AC]/[DA-N_3] ratio on the nonlinear mechanics of the hydrogels, the same prestress protocol at 20 °C was applied to gels of Figure 3B. Figure 6C–E clearly show that increasing the ratio of PNIPAM-AC to DA-N_3 at a fixed concentration of PDA (15 mg mL^{-1}) extends the range of nonlinear deformation, resulting in a concomitant increase of the stiffening factor from 3.5 at a ratio of [PNINAM-AC]/[DA-N_3] = 0.15 up to 7.7 at [PNINAM-AC]/[DA-N_3] = 1.5 (in Figure 6E). This supports the notion that at higher PNIPAM to fiber ratios enhanced intrafiber cross-linking reinforces the fibers and extends the range of nonlinear deformation, as has recently been reported by us by making use of multiarm cross-linkers.[41]

The nonlinear mechanics of physical networks were also studied in comparison to their covalently cross-linked counterparts. Thus, hydrogels from Figure 4B,D were subjected to a range of steady prestress after heating to 55 °C and cooling back to 20 °C (Figure S11). Strikingly, the hydrophobic connections holding the physical gel together were strong enough to support a regime of nonlinear deformation prior to failure. However, both plateau modulus and stiffening factor were substantially lower than in the cross-linked material owing to a lower network connectivity and weaker connections between fibers, respectively.

Having shown that PDA fibers cross-linked with thermoresponsive PNIPAM-AC exhibit thermo- and mechanoresponsiveness, we set out to study the magnitude of the response of PDA/PNIPAM gels to combined mechanical and thermal stimuli. To this end, we carefully subjected a sample of the hydrogel to a range of applied stresses below σ_{max} while continuously recording K' at different temperatures, both below and above the LCST of PNIPAM-AC. Figure 6F shows that the combination of externally applied shear stress and internally generated contractile forces through PNIPAM-AC collapse triggers a strong response that drives the network from an initial soft state with an associated modulus of 1.5 Pa at 20 °C to a final modulus of 2000 Pa at 55 °C just before failure.

CONCLUSIONS

We have shown that chemical cross-linking of semiflexible PDA fibers with a polymer exhibiting LSCT behavior endows the resultant hydrogels with thermo- and stress-responsiveness. The coil-to-globule transition of PNIPAM-AC induces internal stress within the PDA semiflexible fibrous matrix that drives the system into a stressed regime with an associated network stiffening by up to 1000 times its room-temperature linear modulus. The coil-to-globule transition of the linker rigidifies a previously fluid PDA network to rapidly form elastic, strain-stiffening hydrogels. This holds promise in the biomedical field, where it opens the door to their use as injectable materials that quickly form biomimetic scaffolds at body temperature provided that alternative strategies to cross-link PDA fibers avoiding the use of cytotoxic Cu(I) are explored, such as strain-promoted, cycloaddition reactions.[46,47] In addition, promising results have recently emerged making use of analogous bolaamphiphilic constructs as viable materials to support stem cell growth.[48]

We have also shown that the so-formed hydrogels show quantitative resemblance to biological systems in the nonlinear stiffening regime featuring an exponential relationship of the differential modulus with stress that directly mimics the stiffening of collagen gels and, most notably, of reconstituted, active actin/myosin II networks and fibroblast subjected to mechanical prestress. Ultimately, we have illustrated the power and versatility of internally generated forces to enhance the mechanical response of soft materials constructed from entirely man-made building blocks, allowing us to emulate complex biomechanical functions.

ASSOCIATED CONTENT

Supporting Information

The Supporting Information is available free of charge on the ACS Publications website at DOI: 10.1021/jacs.8b10659.

Additional information (PDF)

AUTHOR INFORMATION

Corresponding Author

*r.p.sijbesma@tue.nl

ORCID

Robert Göstl: 0000-0002-7483-6236

Ilja K. Voets: 0000-0003-3543-4821

Rint P. Sijbesma: 0000-0002-8975-636X

Present Addresses

[#]Robert Göstl: DWI - Leibniz Institute for Interactive Materials, Forckenbeckstraße 50, 52056 Aachen, Germany.

[¶]Huda Shaikh: School of Chemistry, University of Bristol, Bristol BS8 1TS, United Kingdom.

Funding

M.F.-C.R. was financially supported by the Marie Curie FP7 SASSYPOL ITN program (No. 607602). R.G. was supported by the Deutsche Forschungsgemeinschaft (DFG) through a research fellowship (GO 2634/1-1.). I.K.V. was financially supported by The Netherlands Organization for Scientific Research (NWO VIDI grant 723.014.006). This work was supported by the Dutch Ministry of Education, Culture and Science (Gravity program 024.001.035).

Notes

The authors declare no competing financial interest.

ACKNOWLEDGMENTS

We thank Dr. K. Pieterse (ICMS Animation Studio) for help with the graphics, Dr. A. W. Bosman of SupraPolix BV for support and fruitful discussions, and Dr. Ir. R. M. Cardinaels (Eindhoven University of Technology) for assistance with the rheological measurements.

REFERENCES

(1) Pollard, T. D.; Borisy, G. G. Cellular Motility Driven by Assembly and Disassembly of Actin Filaments. *Cell* **2003**, *112* (4), 453–465.

(2) Swaney, K. F.; Huang, C.-H.; Devreotes, P. N. Eukaryotic Chemotaxis: A Network of Signaling Pathways Controls Motility, Directional Sensing, and Polarity. *Annu. Rev. Biophys.* **2010**, *39* (1), 265–289.

(3) Windoffer, R.; Beil, M.; Magin, T. M.; Leube, R. E. Cytoskeleton in Motion: The Dynamics of Keratin Intermediate Filaments in Epithelia. *J. Cell Biol.* **2011**, *194* (5), 669–678.

(4) Gardel, M. L.; Shin, J. H.; MacKintosh, F. C.; Mahadevan, L.; Matsudaira, P. A.; Weitz, D. A. Scaling of F-Actin Network Rheology

DOI: 10.1021/jacs.8b10659
J. Am. Chem. Soc. 2019, 141, 1989–1997

to Probe Single Filament Elasticity and Dynamics. *Phys. Rev. Lett.* **2004**, *93* (18), 188102.
(5) Gardel, M. L.; Nakamura, F.; Hartwig, J. H.; Crocker, J. C.; Stossel, T. P.; Weitz, D. A. Prestressed F-Actin Networks Cross-Linked by Hinged Filamins Replicate Mechanical Properties of Cells. *Proc. Natl. Acad. Sci. U. S. A.* **2006**, *103* (6), 1762−1767.
(6) Ruddies, R.; Goldmann, W. H.; Isenberg, G.; Sackmann, E. The Viscoelasticity of Entangled Actin Networks: The Influence of Defects and Modulation by Talin and Vinculin. *Eur. Biophys. J.* **1993**, *22* (5), 309−321.
(7) Gardel, M. L.; Shin, J. H.; MacKintosh, F. C.; Mahadevan, L.; Matsudaira, P.; Weitz, D. A. Elastic Behavior of Cross-Linked and Bundled Actin Networks. *Science* **2004**, *304* (5675), 1301−1305.
(8) Yao, N. Y.; Broedersz, C. P.; Lin, Y.-C.; Kasza, K. E.; MacKintosh, F. C.; Weitz, D. A. Elasticity in Ionically Cross-Linked Neurofilament Networks. *Biophys. J.* **2010**, *98* (10), 2147−2153.
(9) Fletcher, D. A.; Mullins, R. D. Cell Mechanics and the Cytoskeleton. *Nature* **2010**, *463* (7280), 485−492.
(10) Toyota, T.; Head, D. A.; Schmidt, C. F.; Mizuno, D. Non-Gaussian Athermal Fluctuations in Active Gels. *Soft Matter* **2011**, *7* (7), 3234−3239.
(11) Brangwynne, C. P.; Koenderink, G. H.; MacKintosh, F. C.; Weitz, D. A. Nonequilibrium Microtubule Fluctuations in a Model Cytoskeleton. *Phys. Rev. Lett.* **2008**, *100* (11), 118104.
(12) Mizuno, D.; Tardin, C.; Schmidt, C. F.; MacKintosh, F. C. Nonequilibrium Mechanics of Active Cytoskeletal Networks. *Science* **2007**, *315* (5810), 370−373.
(13) Koenderink, G. H.; Dogic, Z.; Nakamura, F.; Bendix, P. M.; MacKintosh, F. C.; Hartwig, J. H.; Stossel, T. P.; Weitz, D. A. An Active Biopolymer Network Controlled by Molecular Motors. *Proc. Natl. Acad. Sci. U. S. A.* **2009**, *106* (36), 15192−15197.
(14) Saez, A.; Ghibaudo, M.; Buguin, A.; Silberzan, P.; Ladoux, B. Rigidity-Driven Growth and Migration of Epithelial Cells on Microstructured Anisotropic Substrates. *Proc. Natl. Acad. Sci. U. S. A.* **2007**, *104* (20), 8281−8286.
(15) Jawerth, L.; Muenster, S.; Weitz, D. A. The Mechanical Mechanism of Platelet Induced Clot Stiffening. *Biophys. J.* **2013**, *104* (2), 150a.
(16) Lacolley, P.; Regnault, V.; Segers, P.; Laurent, S. Vascular Smooth Muscle Cells and Arterial Stiffening: Relevance in Development, Aging, and Disease. *Physiol. Rev.* **2017**, *97* (4), 1555−1617.
(17) Alvarado, J.; Sheinman, M.; Sharma, A.; MacKintosh, F. C.; Koenderink, G. H. Molecular Motors Robustly Drive Active Gels to a Critically Connected State. *Nat. Phys.* **2013**, *9* (9), 591−597.
(18) Weirich, K. L.; Banerjee, S.; Dasbiswas, K.; Witten, T. A.; Vaikuntanathan, S.; Gardel, M. L. Liquid Behavior of Cross-Linked Actin Bundles. *Proc. Natl. Acad. Sci. U. S. A.* **2017**, *114* (9), 2131−2136.
(19) Rachev, A.; Hayashi, K. Theoretical Study of the Effects of Vascular Smooth Muscle Contraction on Strain and Stress Distributions in Arteries. *Ann. Biomed. Eng.* **1999**, *27* (4), 459−468.
(20) Cudjoe, E.; Khani, S.; Way, A. E.; Hore, M. J. A.; Maia, J.; Rowan, S. J. Biomimetic Reversible Heat-Stiffening Polymer Nanocomposites. *ACS Cent. Sci.* **2017**, *3* (8), 886−894.
(21) Storm, C.; Pastore, J. J.; MacKintosh, F. C.; Lubensky, T. C.; Janmey, P. A. Nonlinear Elasticity in Biological Gels. *Nature* **2005**, *435* (7039), 191−194.
(22) Fernandez-Castano Romera, M.; Lafleur, R. P. M.; Guibert, C.; Voets, I. K.; Storm, C.; Sijbesma, R. P. Strain Stiffening Hydrogels through Self-Assembly and Covalent Fixation of Semi-Flexible Fibers. *Angew. Chem., Int. Ed.* **2017**, *56* (30), 8771−8775.
(23) Pal, A.; Voudouris, P.; Koenigs, M. M. E.; Besenius, P.; Wyss, H. M.; Degirmenci, V.; Sijbesma, R. P. Topochemical Polymerization in Self-Assembled Rodlike Micelles of Bisurea Bolaamphiphiles. *Soft Matter* **2014**, *10* (7), 952−956.
(24) Hong, V.; Presolski, S. I.; Ma, C.; Finn, M. G. Analysis and Optimization of Copper-Catalyzed Azide−Alkyne Cycloaddition for Bioconjugation. *Angew. Chem., Int. Ed.* **2009**, *48* (52), 9879−9883.
(25) Geng, J.; Lindqvist, J.; Mantovani, G.; Haddleton, D. M. Simultaneous Copper(I)-Catalyzed Azide−Alkyne Cycloaddition (CuAAC) and Living Radical Polymerization. *Angew. Chem., Int. Ed.* **2008**, *47* (22), 4180−4183.
(26) Schild, H. G.; Tirrell, D. A. Microcalorimetric Detection of Lower Critical Solution Temperatures in Aqueous Polymer Solutions. *J. Phys. Chem.* **1990**, *94* (10), 4352−4356.
(27) Jain, K.; Vedarajan, R.; Watanabe, M.; Ishikiriyama, M.; Matsumi, N. Tunable LCST Behavior of Poly(N -Isopropylacrylamide/Ionic Liquid) Copolymers. *Polym. Chem.* **2015**, *6* (38), 6819−6825.
(28) Brazel, C. S.; Peppas, N. A. Synthesis and Characterization of Thermo- and Chemomechanically Responsive Poly(N-Isopropylacrylamide-Co-Methacrylic Acid) Hydrogels. *Macromolecules* **1995**, *28* (24), 8016−8020.
(29) Head, D. A.; Levine, A. J.; MacKintosh, F. C. Deformation of Cross-Linked Semiflexible Polymer Networks. *Phys. Rev. Lett.* **2003**, *91* (10), 108102.
(30) Onck, P. R.; Koeman, T.; van Dillen, T.; van der Giessen, E. Alternative Explanation of Stiffening in Cross-Linked Semiflexible Networks. *Phys. Rev. Lett.* **2005**, *95* (17), 178102.
(31) Chen, P.; Shenoy, V. B. Strain Stiffening Induced by Molecular Motors in Active Crosslinked Biopolymer Networks. *Soft Matter* **2011**, *7* (2), 355−358.
(32) Lam, W. A.; Chaudhuri, O.; Crow, A.; Webster, K. D.; Li, T.-D.; Kita, A.; Huang, J.; Fletcher, D. A. Mechanics and Contraction Dynamics of Single Platelets and Implications for Clot Stiffening. *Nat. Mater.* **2011**, *10* (1), 61.
(33) Broedersz, C. P.; MacKintosh, F. C. Molecular Motors Stiffen Non-Affine Semiflexible Polymer Networks. *Soft Matter* **2011**, *7* (7), 3186−3191.
(34) MacKintosh, F. C.; Levine, A. J. Nonequilibrium Mechanics and Dynamics of Motor-Activated Gels. *Phys. Rev. Lett.* **2008**, *100* (1), 018104.
(35) Liverpool, T. B.; Marchetti, M. C.; Joanny, J.-F.; Prost, J. Mechanical Response of Active Gels. *EPL* **2009**, *85* (1), 18007.
(36) Fernández-Castaño Romera, M.; Lou, X.; Schill, J.; ter Huurne, G.; Fransen, P.-P. K. H.; Voets, I. K.; Storm, C.; Sijbesma, R. P. Strain-Stiffening in Dynamic Supramolecular Fiber Networks. *J. Am. Chem. Soc.* **2018**, *140*, 17547.
(37) Hammouda, B.; Ho, D. L.; Kline, S. Insight into Clustering in Poly(Ethylene Oxide) Solutions. *Macromolecules* **2004**, *37* (18), 6932−6937.
(38) Hule, R. A.; Nagarkar, R. P.; Hammouda, B.; Schneider, J. P.; Pochan, D. J. Dependence of Self-Assembled Peptide Hydrogel Network Structure on Local Fibril Nanostructure. *Macromolecules* **2009**, *42* (18), 7137−7145.
(39) Broedersz, C. P.; Kasza, K. E.; Jawerth, L. M.; Münster, S.; Weitz, D. A.; MacKintosh, F. C. Measurement of Nonlinear Rheology of Cross-Linked Biopolymer Gels. *Soft Matter* **2010**, *6* (17), 4120−4127.
(40) Jaspers, M.; Dennison, M.; Mabesoone, M. F. J.; MacKintosh, F. C.; Rowan, A. E.; Kouwer, P. H. J. Ultra-Responsive Soft Matter from Strain-Stiffening Hydrogels. *Nat. Commun.* **2014**, *5*, 5808.
(41) Kouwer, P. H. J.; Koepf, M.; Le Sage, V. A. A.; Jaspers, M.; van Buul, A. M.; Eksteen-Akeroyd, Z. H.; Woltinge, T.; Schwartz, E.; Kitto, H. J.; Hoogenboom, R.; et al. Responsive Biomimetic Networks from Polyisocyanopeptide Hydrogels. *Nature* **2013**, *493* (7434), 651−655.
(42) MacKintosh, F. C.; Käs, J.; Janmey, P. A. Elasticity of Semiflexible Biopolymer Networks. *Phys. Rev. Lett.* **1995**, *75* (24), 4425−4428.
(43) Lin, Y.-C.; Yao, N. Y.; Broedersz, C. P.; Herrmann, H.; MacKintosh, F. C.; Weitz, D. A. Origins of Elasticity in Intermediate Filament Networks. *Phys. Rev. Lett.* **2010**, *104* (5), 058101.
(44) Fernández, P.; Pullarkat, P. A.; Ott, A. A Master Relation Defines the Nonlinear Viscoelasticity of Single Fibroblasts. *Biophys. J.* **2006**, *90* (10), 3796−3805.

DOI: 10.1021/jacs.8b10659
J. Am. Chem. Soc. 2019, 141, 1989−1997

(45) Licup, A. J.; Münster, S.; Sharma, A.; Sheinman, M.; Jawerth, L. M.; Fabry, B.; Weitz, D. A.; MacKintosh, F. C. Stress Controls the Mechanics of Collagen Networks. *Proc. Natl. Acad. Sci. U. S. A.* **2015**, *112* (31), 9573−9578.
(46) Agard, N. J.; Prescher, J. A.; Bertozzi, C. R. A Strain-Promoted [3 + 2] Azide−Alkyne Cycloaddition for Covalent Modification of Biomolecules in Living Systems. *J. Am. Chem. Soc.* **2004**, *126* (46), 15046−15047.
(47) Dommerholt, J.; Rutjes, F. P. J. T.; van Delft, F. L. Strain-Promoted 1,3-Dipolar Cycloaddition of Cycloalkynes and Organic Azides. *Top. Curr. Chem.* **2016**, *374* (2), 16.
(48) Tong, C.; Liu, T.; Saez Talens, V.; Noteborn, W. E. M.; Sharp, T. H.; Hendrix, M. M. R. M.; Voets, I. K.; Mummery, C. L.; Orlova, V. V.; Kieltyka, R. E. Squaramide-Based Supramolecular Materials for Three-Dimensional Cell Culture of Human Induced Pluripotent Stem Cells and Their Derivatives. *Biomacromolecules* **2018**, *19* (4), 1091−1099.

DOI: 10.1021/jacs.8b10659
J. Am. Chem. Soc. 2019, 141, 1989−1997